Tribology International 44 (2011) 820–828

Friction and wear behaviours of Ti(C,O,N) dark decorative coatings

D. Munteanu [a,*], C. Gabor [a], D.G. Constantin [a], B. Varga [a], R. Adochite [a], O.C. Andrei [b], J.M. Chappé [c], L. Cunha [c], C. Moura [c], F. Vaz [c]

[a] Department of Technological Equipment and Materials Science, Transilvania University, 500036 Brasov, Romania
[b] Department of Removable Partial Denture, University Carol Davila, 020022 Bucharest, Romania
[c] Centre of Physics, Minho University, Azurém Campus, 4800-058 Guimarães, Portugal

A B S T R A C T

Reactive magnetron sputtering was used to obtain dark Ti(C,O,N) decorative coatings onto high speed steel. From a crystallographic point of view, depending by the amount of (N+O) mixture, the obtained films could be divided in two major regions: the first one with a predominant fcc crystallographic structure (for low amounts of (N+O)), and the second one containing films with amorphous structures. The best results for friction coefficient and wear rates (the minimum values) were registered for samples prepared in the beginning of the amorphous region. These two tribological parameters are mainly influenced by the carbon content in the films. Taking into account the practical goal of these kinds of films, the pure black films were obtained for higher amount of (N+O) mixture. Also for these amorphous darkest films reached in oxygen and nitrogen, the tribological properties are acceptable and the adherence reaches the maximum value.

1. Introduction

Decorative thin films are used for a long time and their commercial importance is increasing, particularly concerning high quality products. Besides the attractive colours, the decorative coatings must supply surface quality, skin compatibility, high wear resistance and protection against corrosion. Latest technology may allow producing thin films with a wide range of colours, intrinsic or by interference. Beyond the well known golden colours achieved by TiN and ZrN, transition metal oxynitride thin films (titanium, zirconium, etc.) are used to get brown, golden, green, purplish-pink, blue or violet tones [1–4]. Although it is known that black colour on thin films is relatively hard to obtain and that in most cases only tones of dark grey or brown are achieved, certain black coatings have been obtained: Cu–Ni films deposited by electrochemical deposition [5], Ni–P alloys by electroless plating [6] and Ti–N–(C,Al) [7] or amorphous carbon coatings by sputtering [8]. However none of these studies presented more than one black tone. As far as it is known, except a previous work of the authors of this paper, only a few publications were done on this system [9–13] and none of them focuses on the colours of these Ti(C,O,N) films.

In terms of tribological characterisation, it is worth to mention that TiC and TiN films have been studied by many authors [14–16] due to their low friction coefficient, high hardness and wear resistance [17–21]. It must be also mentioned, that TiC can present brittle fractures due to its brittleness, while TiN is limited by its relatively low hardness [22]. Therefore, a derived coating with improved performances was studied, namely the TiCN films, that posses high hardness, better toughness and lower friction coefficient than TiC and TiN [23]. Furthermore, it was proved that oxygen is a good candidate for the improvement of films properties [24]. Many authors [11,25–32] described the positive influence of oxygen on material's properties, due to the small atomic size of oxygen and its reactivity [11,25]. Oxygen allows to obtain a wide spread of properties (including optical ones, such as film's colour) while keeping good mechanical and tribological properties [26,32]. On the other hand, it is known that Ti–O coatings have the possibility to form magnelis-phase (TiO_{2-x}), which is known to have very low friction coefficients [20]. There is also the possibility to form a nc-TiC phase and an amorphous phase (a-C or a-TiO_x) [20,33]. These aspects induce that Ti(C,O) films can be very good candidates for tribological applications.

Concerning the Ti(N,O) thin films, an important scientific interest [34,35] can be observed, mainly because it benefits from metallic oxides properties (colour, optical properties) and nitrides ones (hardness or wear resistance) [36]. This combination of properties can be achieved by tailoring the N/O ratio. Taking into account all these facts, the addition of carbon to Ti(N,O) thin films allowed obtaining good mechanical properties together with a brilliant black colour, as it was in fact expected.

The work described in this paper deals with the deposition and characterisation of Ti(C,O,N) decorative coatings by reactive magnetron sputtering. The goals are to produce coatings in an

* Corresponding author. Tel./fax: +40 268 411877.
E-mail addresses: munteau.d@unitbv.ro, danielmunteanu@hotmail.com (D. Munteanu).

0301-679X/$ - see front matter © 2011 Elsevier Ltd. All rights reserved.
doi:10.1016/j.triboint.2011.02.004

economical mode with several black tones and to find certain compositions with acceptable mechanical and tribological properties. In the case of this work, only one chamber configuration was used with one Ti solid target and three reactive gases: acetylene and a mixture of nitrogen and oxygen. This system allowed obtaining very dark attractive colours. The mechanical and tribological properties were correlated to the atomic composition and the crystallographic structure.

2. Experimental details

The Ti(C,O,N) thin films were deposited onto high speed steel (AISI M2) and silicon substrates in a custom-made dc reactive magnetron sputtering apparatus. The films were prepared with the substrate holder positioned at 70 mm in all runs, using a current density of 100 A m^{-2} on the titanium target (99.6 at% purity). A gas atmosphere composed of argon (working gas), nitrogen+oxygen (17:3 ratio) reactive mixture and acetylene were used for the depositions. The argon flow was fixed at 60 sccm in all depositions. The flow rate of the reactive gas mixture (O_2+N_2) varied from 2 to 18 sccm and the acetylene flow was kept constant at 5 sccm. The working pressure was approximately constant at 0.35 Pa and the substrates were grounded. During the 1 h depositions the temperature was kept constant at 200 °C, using an external heating resistance. The atomic composition of the as deposited samp1es was measured by electron probe microanalysis (EPMA) in a Cameca SX-50 apparatus. The film's thickness was measured by CALOTEST method (CSM Instruments). The structure of the films was analysed by X-ray diffraction (XRD) on using the Co Kα radiation (λ=0.1788 nm) of a Siemens D—500 apparatus, in Bragg–Brentano configuration [13]. The coated samples used for XRD were prepared on silicon (1 0 0) substrate, at the same time and conditions with the steel substrate samples.

Film's hardness and Young's modulus were determined from the loading and unloading curves, carried out with an ultra low load-depth sensing Berkovich nanoindenter from CSM Instruments. The maximum load used was 30 mN, with a loading time of 30 s, holding of 30 s and unloading of 30 s, producing an average number of 15 indentations per sample.

The dynamic friction coefficient and wear rate values (abrasion wear) were estimated using a ball-on-disc tribosystem (CSM Instruments). The static partner (the counter-body), a 6 mm diameter steel ball (AISI 100Cr6) hardened and low tempered, with a final hardness of 62 HRC, was mounted on a stiff lever, designed as a frictionless force transducer. During the sample rotation, the frictional forces acting between the ball and sample are measured by very small deflections of the lever using an LVDT sensor. This sensor measures the tangential force F_t and provides then the friction coefficient (dynamic friction coefficient). A schematic arrangement of the tribosystem is given in Fig. 1.

The adhesion/cohesion of the coatings was evaluated by scratch-testing technique using a Revetest, (CSM Instruments). The load was increased linearly from 0 to 50 N (Rockwell C 200 μm radius indenter tip, loading speed of 10 N/min and scratch speed of 1 mm/min). The critical loads L_c values corresponding to the adhesive failure mechanisms were measured by analysing the failures events in the scratch track by optical microscopy. Regarding to the critical loads L_c, it has been taken into consideration all the three parameters L_{c1}, L_{c2} and L_{c3}, which represent the load corresponding to apparition of the first cracking (L_{c1}), the load for first delamination (L_{c2}) and the load for full delamination (L_{c3}).

Wear rates for each sample are calculated from the volume of material lost during a specific friction run. This simple method

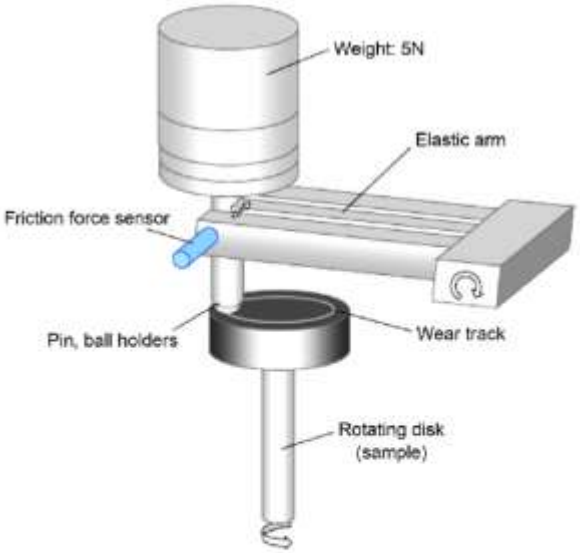

Fig. 1. Schematic arrangement of the tribosystem.

facilitates the determination and study of friction and wear behaviour of the samples. The calculation of the worn track section for each sample was also done using a profilometer, Taylor Hobson type. For all wear tests, the annular type wear surface was characterised by a radius of 9 mm. In fact, by help of the TriboX Software (CSM Instruments), it has been calculated for each sample the volume of material lost after the wear test, taking into account the transversal area of the worn track, the length of it (the length of circular channel obtained in depth, on the sample surface) and the applied load.

Taking into account that the main practical aim of these kinds of coatings is the decorative functional character, the normal load applied by the ball on the sample surface was 5 N and the maximum number of laps was 450. The linear speed of the rotating plateau was 4.8 cm s^{-1}. These values were in accordance with our previous experience in testing decorative coatings. Before all the wear tests, the samples, the sliding half-couples and the balls were cleaned with isopropanol. The environmental conditions for all tribological tests were: T=24 °C and 30% humidity.

Details on surfaces topography features of the films (R_q—root mean square deviation of the assessed profile) were studied by atomic force microscopy (AFM).

The decorative aspects of these films where studied by J.M. Chappé et al. [13]. Film's colour was computed by spectrophotometery. Colour specification was represented under the standard CIE illuminant D65 (specular component excluded) and represented in the CIELAB 1976 colour space [37,38]. The coatings reflectance was measured by UV–vis spectroscopy.

3. Results and discussion

3.1. Compositional and structural features

Table 1 presents a summary of all prepared samples with deposition conditions and resulting compositions.

According to Table 1, the Ti concentrations varied between 18.7 at% (sample S3—$TiC_{1.01}O_{0.80}N_{1.63}$) and 38.4 at% (sample S1—$TiC_{0.78}O_{0.31}N_{0.51}$) and C between 17.6 at% (sample S8—$TiC_{0.77}$

Table 1
Summary of the films peepared within the framework of this paper.

Sample	Gas flows (sccm)			Atomic formula	Composition (at%)			
	C_2H_2	N_2+O_2	Ar		Ti	C	N	O
S1	5	2	60	$TiC_{0.78}O_{0.31}N_{0.51}$	38.4	30.0	19.7	11.9
S2	5	4	60	$TiC_{1.03}O_{0.57}N_{1.04}$	27.4	28.4	28.5	15.7
S3	5	8	60	$TiC_{1.91}O_{0.80}N_{1.63}$	18.7	35.8	30.6	14.9
S4	5	10	60	$TiC_{1.81}O_{1.79}N_{1.61}$	19.4	35.1	31.2	14.3
S5	5	12	60	$TiC_{1.55}O_{1.85}N_{1.70}$	19.5	30.3	33.2	17.0
S6	5	14	60	$TiC_{1.36}O_{1.10}N_{1.57}$	19.8	27.2	31.2	21.8
S7	5	16	60	$TiC_{1.39}O_{1.02}N_{1.76}$	19.7	25.6	34.7	20.0
S8	5	18	60	$TiC_{0.77}O_{1.20}N_{1.37}$	23.0	17.6	31.7	27.7

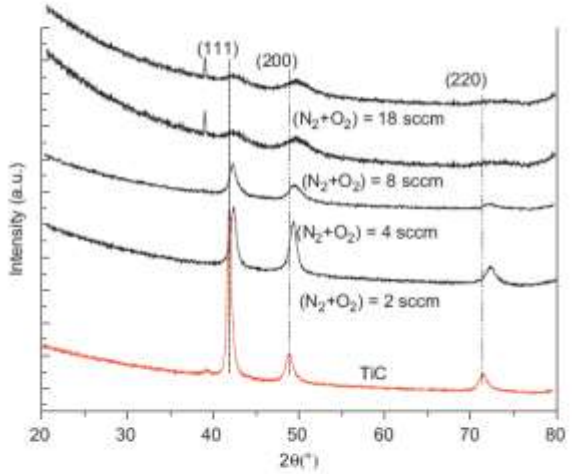

Fig. 2. XRD diffractograms of the prepared films for different reactive gas flows [3].

$O_{1.20}N_{1.37}$) and 35.8 at% (sample S3—$TiC_{1.91}O_{0.80}N_{1.63}$). Except for sample S1, where the N concentration is relatively low (19.7 at%), the overall samples present concentrations of this element around 30 at%. O is minimal for sample S1 (11.9 at%) and maximal for sample S8 (27.7 at%).

Taking into account the ratio values between the whole amount of non-metallic elements and titanium, all the obtained compounds could be considered in over-stoechiometric form. These values of (C+O+N)/Ti ratio are comprised between 1.60 for the sample S1 ($TiC_{0.78}O_{0.31}N_{0.51}$) with the maximum amount of Ti and 4.34 for the sample S3 ($TiC_{1.91}O_{0.80}N_{1.63}$) with maximum amount of C. If we consider the variation of (N_2+O_2) gas flow (Table 1), these extreme values are placed in a small interval, 2–8 sccm. These composition differences and the variation of nitrogen and oxygen amounts, respectively, lead to different grey colour tones for the obtained films.

What it has to be underline here is the fact that, from a decorative goal point of view, the black tones have been obtained starting with sample S2 ($TiC_{1.03}O_{0.57}N_{1.04}$). All the samples after S2 (includind it also) could be considered as black for a human observer. However, the samples with the highest content of oxygen present the best colorimetric characteristics to be considered as black. This is an important reason from a practical point of view, to be taken into consideration for mechanical and tribological characterisation.

XRD patterns (Fig. 2) of the deposited films revealed a strong dependence of the film texture on the gas mixture flow rate, as well as on the atomic composition. Taking into account the XRD results and reporting to the typical diffraction patterns of fcc TiC-like films, the Ti(C,O,N) films prepared at low partial pressure values (low mixture gas flows, 2–4 sccm), exhibit peaks shifted to higher diffraction angles, which may induce the conclusion that the films exhibit a titanium carbide-type cubic structure, with inclusion of oxygen and/or nitrogen atoms ($TiC_x(O,N)$). This kind of stucture would be very closer to others formed on the basis of TiC, TiN or TiO types, which have similar lattice parameters (TiC = 0.4328 nm from JCPDS04-004-2919, TiN = 0.4241 nm from JCPDS04-001-2271 and TiO = 4177 nm from JCPDS04-001-6834). Furthermore, the diffraction peaks become less intense and almost disappear for (N_2+O_2) gas flows higher than 8 sccm (Fig. 2). This films zone limit corresponds to the transition into the films amorphous region. Thus, from a structural point of view, we can discuss about two main regions, the cristalline one (samples S1 and S2) and the amorphous one (the rest of the samples).

The crystalline films are those located in the first region ($N_2+O_2 < 4$ sccm), where the composition of the films is sub- to roughly stoichiometric ((N+O+C)/Ti roughly higher than 0.7). According to [13], the slight decrease of the carbon content, for $N_2+O_2 \leq 4$ sccm, may be related with the lowest value of standard enthalpy of formation for TiC. The fact that the ratio N+O+C over Ti is increasing rapidly above 1 ($N_2+O_2 > 4$ sccm) makes the films pass from a situation where almost all arriving species are added to the growing film (first zone), to a zone where the excess of N+O+C in respect to Ti is most likely inducing some preferential reactions of Ti, according to the reactivity of each reactive gas. In the second region, the films lose their long range order, which may result from the joined effects of both low surface diffusion of the particles impinging on the substrate or the growing film (the depositions were made at only 200 °C), and the significant over-stoichiometric condition of the films (Ti is only around 20 at% within the higher N_2+O_2 flows zone).

The standard enthalpies of formation of TiC, TiN, TiO and TiO_2 compounds are respectively, −184, −338, −520 and −942 kJ mol^{-1}. This higher affinity of titanium towards oxygen induces much higher oxygen content in the film than the one expected from the gas mixture [13]. Thus, there is the possibility for developing poorly crystallised oxide structures and this is important to keep in mind for further explanations.

3.2. Thickness and deposition rate

The film's thickness after 1 h deposition varied between 1.25 and 1 μm (Table 2), which means that also the deposition known a small decreasing with increase of reactive gas mixture (O_2+N_2) flow. We could discuss about a stabilisation of the deposition rate at lower values, especially in the amorphous structural regime. This aspect is sustained also by the target voltage evolution, which had a high value at the beginning (around of 530 V), known a decrease for reactive gas flows between 4 and 10 sccm, (between 470 and 500 V), and again, an increasing and stabilisation to 537 V for more than 10 sccm. The first decreasing occurs do to the metallic regime of deposition and surface target composition modification and the reduction of the ion induced secondary electron emission (ISEE) coefficient.

If the reactive gas flow increase, we could discuss on the possibility for non-reacted oxygen/nitrogen on the target surface. The increase of the contamination film thickness on the target surface decreases the electrical conductivity of the target. Therefore a higher cathode potential is necessary to break this insulating barrier on the target (the apparition of poisoning effect).

3.3. Mechanical and tribological behaviours

3.3.1. Hardness and elastic modulus

Table 2 presents the experimental results in terms of thickness and mechanical properties (hardness and elastic modulus). The

Table 2
Thickness and mechanical properties of as deposited coatings.

Sample	Thickness (μm)	Mechanical properties	
		Hardness (GPa)	Elastic modulus (GPa)
S1	1.25	12.7	159
S2	1.20	10.3	124
S3	1.00	11.3	127
S4	1.00	11.3	133
S5	1.00	8.7	121
S6	1.00	9.1	123
S7	1.00	11.3	150
S8	1.00	10.4	147

hardness presents moderate values, between 8.7 and maximum 12.7 GPa in the first zone—crystalline region, much lower in comparisson with TiC films which can exceed 30 GPa. This important difference could be generated by the over-stoechiometry of the films. This aspect was observed also by our group in others studies, in the case of Ti(C,O) films [20].

The structural changes induced by the oxygen incorporation in the films, seems to be the major responsible of this decrease in hardness, as well as the continuous amorphization tendency that is revealed in the films with increasing of the (O+N)/Ti ratio. The hardness reached a minimum value for S5 sample ($TiC_{1.55}O_{0.87}N_{1.70}$)—8.7 GPa; in terms of composition, this sample (S5) marks the start of decreasing carbon and increasing oxygen in the composition. However, for the highest O contents in the films, there is a slight improvement of hardness; this increase tendency was observed also in [20] and might be related with the formation of poorly crystallised oxide phases.

The hardness evolution can be correlated as well with the elastic modulus values. In fact, there is almost the same evolution of both parameters related to (N_2+O_2) gas flow. The highest values of elastic modulus are registered, of course, in the first zone (the crystalline region), showing a good strength to plastic deformation. Very closed values can be observed also in the amorphous high (O+N) content region (samples S7—$TiC_{1.30}O_{1.02}N_{1.76}$ and S8—$TiC_{0.77}O_{1.20}N_{1.37}$) and, again, this could explain again the good correlation with hardness.

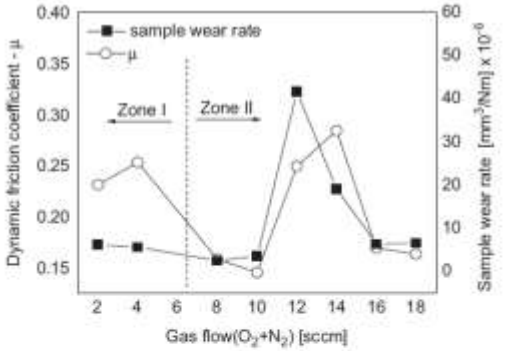

Fig. 3. The influence of reactive gas flow on friction coefficient and wear rate.

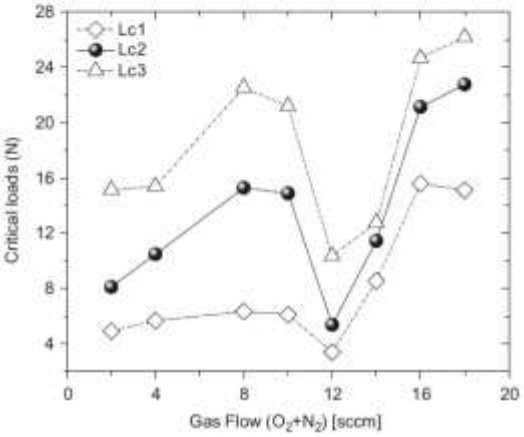

Fig. 4. The influence of reactive gas flow on adherence behaviour.

3.3.2. Friction coefficient, wear rate and adherence

Fig. 3 presents the overall tribological test results, where the dynamic friction coefficient and the wear rate of samples are plotted as a function of the gas flow rate variation. Fig. 4 shows the values of critical loads L_c for each sample and correlation of these with the same variation of the gas flow.

According to these plots, the experimental results show a very good correlation between friction coefficient, wear rate and adherence. Thus, the samples prepared with lower gas flow rates – zone I – reveal moderate values for friction coefficient (arround of 0.24) and lower values for wear rates, corresponding also to the maximum values of hardness and elastic modulus (Table 2), which, by its turn result most probably from the crystalline nature of these samples.

The tribological parameter values reveal some decrease tendency with the structure transformation tendency towards amorphous state (for flows between 8 and 10 sccm). Here it has been registered the minimum values for friction coefficient and wear rate—samples S3 ($TiC_{1.91}O_{0.80}N_{1.63}$) and S4 ($TiC_{1.81}O_{0.73}N_{1.61}$). This behaviour is well correlated with the adherence test results (Fig. 4). An increase of critical load values have been registered here. It is important to be mentioned here that the critical load L_{c1} corresponding to the apparition of the first cracking is reached relatively early, at around 6 N, and this aspect is characteristic to all the samples containing moderate oxygen content (samples from S1 to S5). It means, that the top of the coating seems to be brittle, having a lower toughness.

At the same time, it is very important to remark that the two samples (S3 and S4) are characterised in terms of composition, by maximum amounts of carbon and maximum amounts of non-metalic elements. This high carbon amount could play an important role in the friction–wear process, acting like a solid lubricant.

According to different other researches, increasing the C content and keeping the crystalline structure of cubic TiC lattice, the friction coefficient also decreases [39,40]; these remarks are in accordance with the results for samples S1 and S2. Moreover, for higher amounts of C, the friction coefficient will decrease even more, if the TiC crystallites are embedded in an amorphous C tissue due to the solid lubricant effect of C [41].

Besides the influence of C on the friction behaviour, the decreasing of friction coefficient values in the beginning of the amorphous structural region (samples S3 and S4—Fig. 2) could be sustained also in explanations also by the AFM surface images (Fig. 5a–c).

As it can be observed, there is a clear difference in roughness (R_q) between the predominant crystalline films in the first region (sample S1, R_q = 21 nm—Fig. 4a) and the films in the beginning of

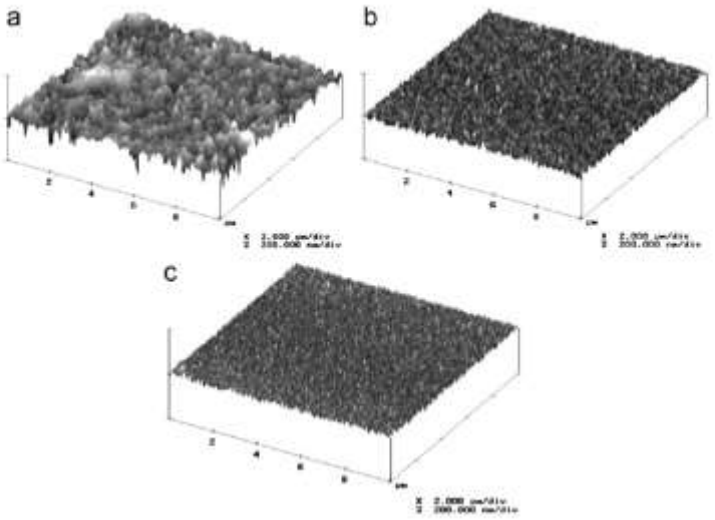

Fig. 5. Surface roughness images obtained by AFM: (a) sample S1 ($TiC_{0.79}O_{0.31}N_{0.51}$) R_q=21 nm; (b) sample S3 ($TiC_{1.01}O_{0.46}N_{1.01}$) R_q=8.7 nm and (c) sample S ($TiC_{1.01}O_{0.73}N_{1.01}$) R_q=6.5 nm.

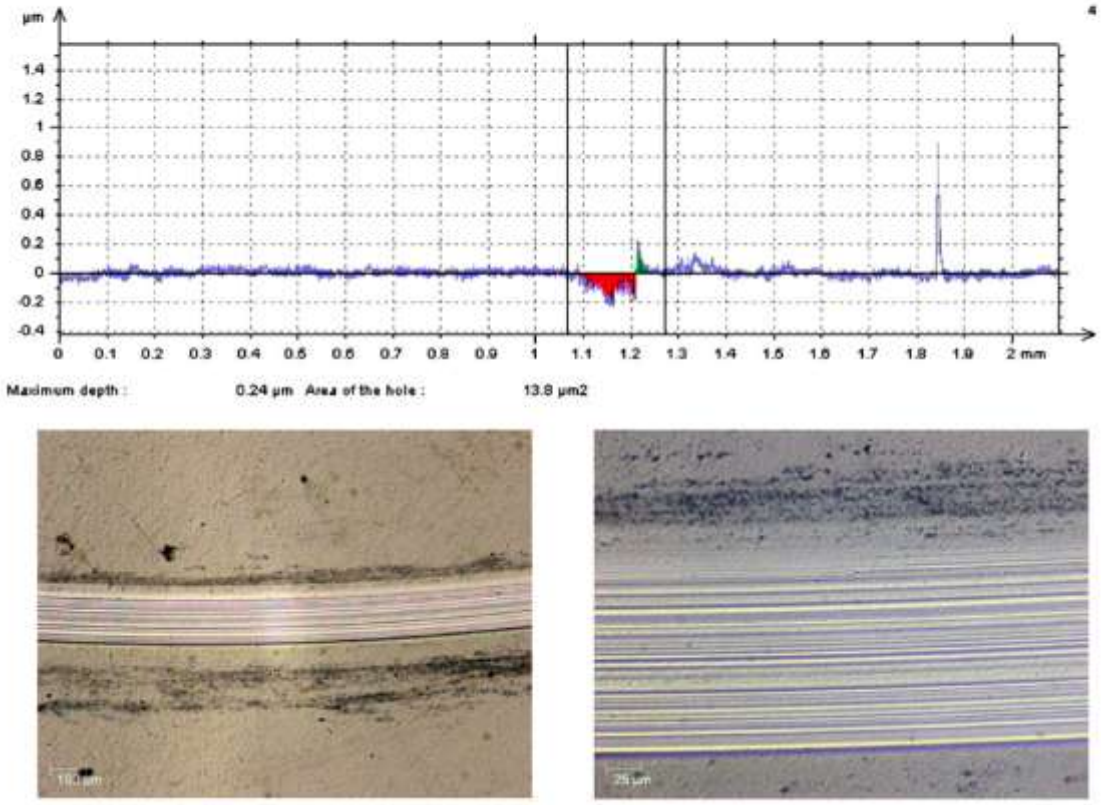

Fig. 6. The wear evaluation for the sample S1—$TiC_{0.79}O_{0.31}N_{0.51}$.

the amorphous region (samples S3, R_q=8.7 nm and S4, R_q=6.5 nm—Fig. 5b and c). In fact, for the samples prepared with reactive mixture flows (N_2+O_2) higher than 10 sccm (starting with S4 sample—$TiC_{1.81}O_{0.73}N_{1.61}$), the R_q roughness values have been kept almost constant, at around 6 nm. The images show that there is notorious tendency for roughness decreasing with the amorphization of the samples. Thus, this decreasing of roughness and the compact aspect of the film could complete the influence of carbon for improving friction conditions.

Beyond the composition related aspects, Gulbinski et al. [40] also revealed that, for TiC crystalline coatings, the increasing of C amount leads to a higher hardness and lower friction coefficients. This decreasing of friction coefficient based on the hardness modification is explained by the reduction of the real contact area and the decrease of surface roughness.

At the same time, and in terms of both tribological parameters (friction coefficient and wear rate), this small difference between the group of the first two samples (in the crystalline region, zone I) and the second group of samples (the third and the fourth, beginning of zone II) could be sustained also by the general friction behaviour during the tests. It was observed a moderate tendency for a brittle tribological behaviour of the samples in the crystalline region generated by the higher hardness.

According to Fig. 6, for the crystalline region, the wear phenomenon in depth of the layer exists at a low level, at about 20% of the coating thickness. With the beginning of amorphous region (samples S3 and S4), the wear track become less deep after the wear test (Fig. 7). At the same time, the transversal area affected by the wear process becomes smaller. The wear proces is developed very superficial and in a streaky form along th circular distance test, on the surface plan. On the sample surface the width of circular wear track becomes smaller. The wear trac is concentrated especially very near to circular track generated by the hertzian contact point, where the contact pressure reached maximum value, but it is present also on one side and on th other side of the central circular track. We could discuss about ar alternating (concentric) aspect of wear and sliding paths. Accord ing to the profilometer testing results, it could be remarked int the transversal area of the sample, certain strait gutters, inside th film thickness.

After this region, there is a pounce both for wear rate an friction coefficient, in the interval of 12–14 sccm. This interva is represented by two samples, S5—$TiC_{1.55}O_{0.87}N_{1.70}$, and S6—$TiC_{1.36}O_{1.10}N_{1.57}$ (Fig. 3). The adherence in this region become worst too (Fig. 4), the registered critical loads having the lowes values. Although the hardness values are not very different for al the samples, one can observe minimum values for these two ones The elastic modulus reached minimum values here too (Table 2)

In terms of deposition parameters, these worse mechanica and tribological behaviours in this region could be correlated wit the evolution of the target potential and the development of io poisoning process. It is possible that in this segment of reactiv gas flow values to register the transition from metallic to oxide nitride regime of deposition. For the moment, here was registere a bounce of the target potential. In fact, when the reactive ga mixture flow and, of course the partial pressure increase, th

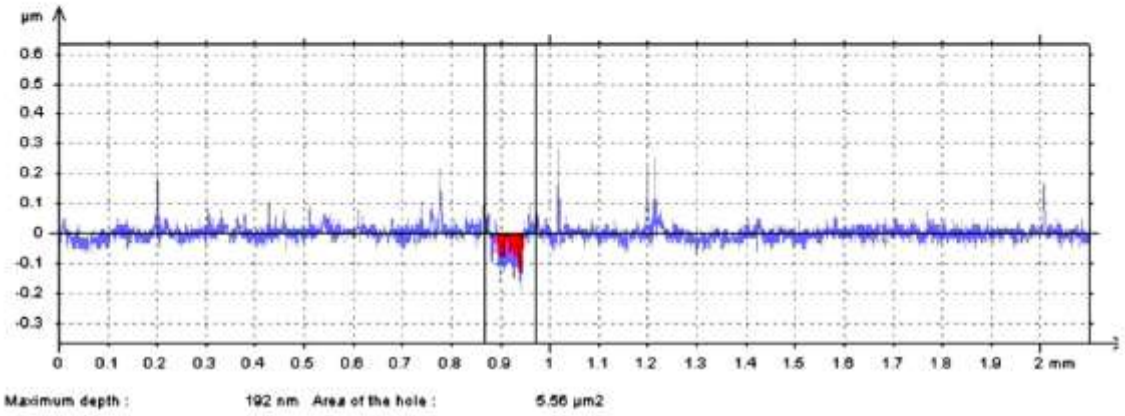

Fig. 7. The wear evaluation for the sample S3—$TiC_{1.36}O_{0.80}N_{1.03}$.

target oxidation (poisoning effect) starts to prevail (resulting from the increased ionisation of these reactive gases, which evolves to their actual dissociation) and hence a contamination layer (oxide/nitride) grows on the target surface.

Regarding the composition, in this interval, the C content of the two samples decreased in comparison with the concentration of samples S3 and S4. Thus, it is credible to affirm that this sudden increasing of friction coefficient and wear rate (for the moment) could be generated firstly, by the lower hardness and adherence of the films, and secondly, by the start of C content decrease, which influenced also the hardness and friction coefficient.

Fig. 8 presents the worst wear behaviour characteristics – sample S5 – $TiC_{1.55}O_{0.87}N_{1.70}$. According to Fig. 8, the wear process affected all the film thickness and also the substrate. It can be observed a severe wear track, revealing a strong friction contact (abrasion wear) between the substrate (steel) and the ball. The wear phenomenon is developed in a uniform manner and it lead to a spalling process of the film. In this case, a large area of substrate is visible. There are also wear debris ingrained on the substrate wear track provided by the blasted film.

With the increasing of (N_2+O_2) flow above 14 sccm, there is a clear tendency for an improvement of the tribological parameters and for a stabilisation at an almost constant level, for both friction coefficient and wear rate (16–18 sccm, samples S7—$TiC_{1.30}O_{1.02}N_{1.76}$ and S8—$TiC_{0.77}O_{1.20}N_{1.37}$) (Fig. 3). At the same time, the adherence knows an improving in this region (Fig. 4). Regarding the adherence, it is important to be mentioned here that the critical load values—L_{c1} for these last two samples are higher in comparison with the rest; this could leads to the conclusion that the films have a higher toughness even in the top of them. Besides L_{c1}, another fact is worth to be mention is the highest critical load values L_{c2} and L_{c3} to these two last samples (S7 and S8). If we take into account the XRD results which revealed an amorphous structures in this region but also the maximum amount of oxygen, we could conclude that these kinds of structures are able to better accommodate the deformations induced by the movement of the scratch tip.

Moreover, if one keeps in mind that in this oxygen reach region there is already some tendency to obtain poorly crystallised oxide structures, this means that the structural features are playing a decisive role for the adhesion behaviour. In fact, if we take into consideration the low friction coefficient of TiO_2 films (arround 0,1 for TiO_2 prepared by sol–gel technique) [42], this possibility for developing Ti–O structures could explain the decreasing of friction coefficient value.

Also to be underlined here is the fact that this good tribological behaviour of the last two samples is not much influenced by the carbon content, which continued to decrease; in opposite, these possible poorly crystallised oxide structures could have a positive influence. At the same time, the hardness and elastic modulus values were high enough on these samples, revealing good elasticity in these films. An alternative striped wear aspect was observed in a transversal image, containing fine wear ditches at

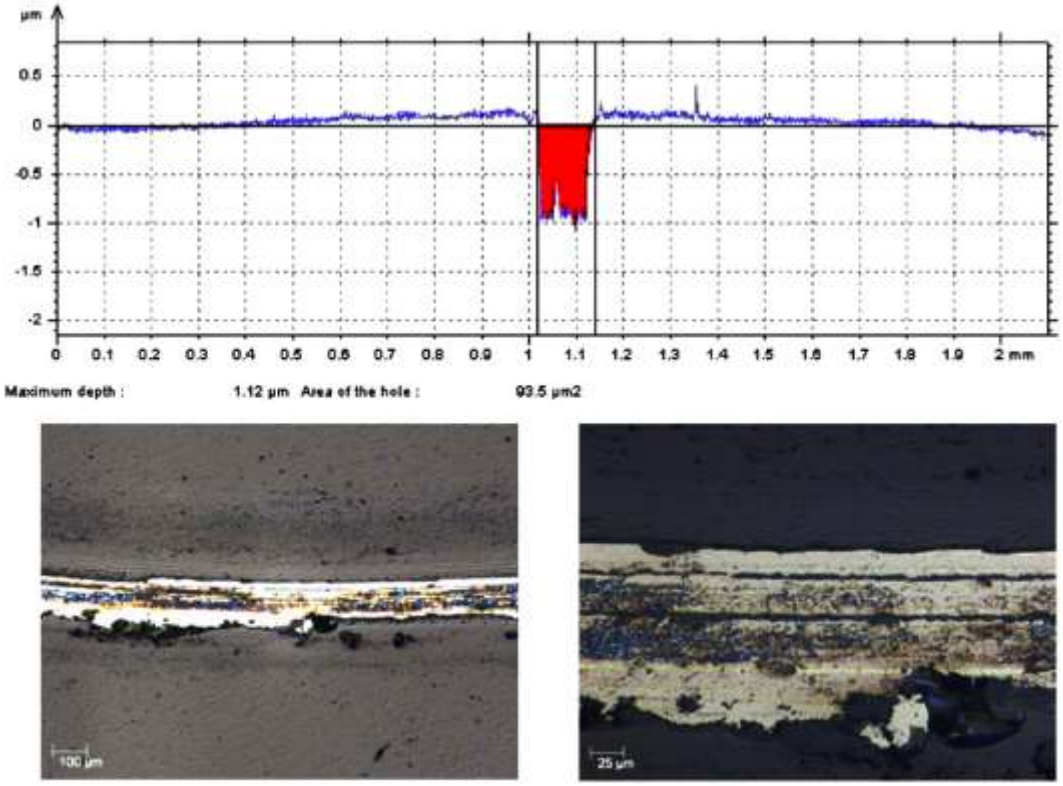

Fig. 8. The worst wear behaviour characteristic of sample S5—$TiC_{1.55}O_{0.87}N_{1.70}$.

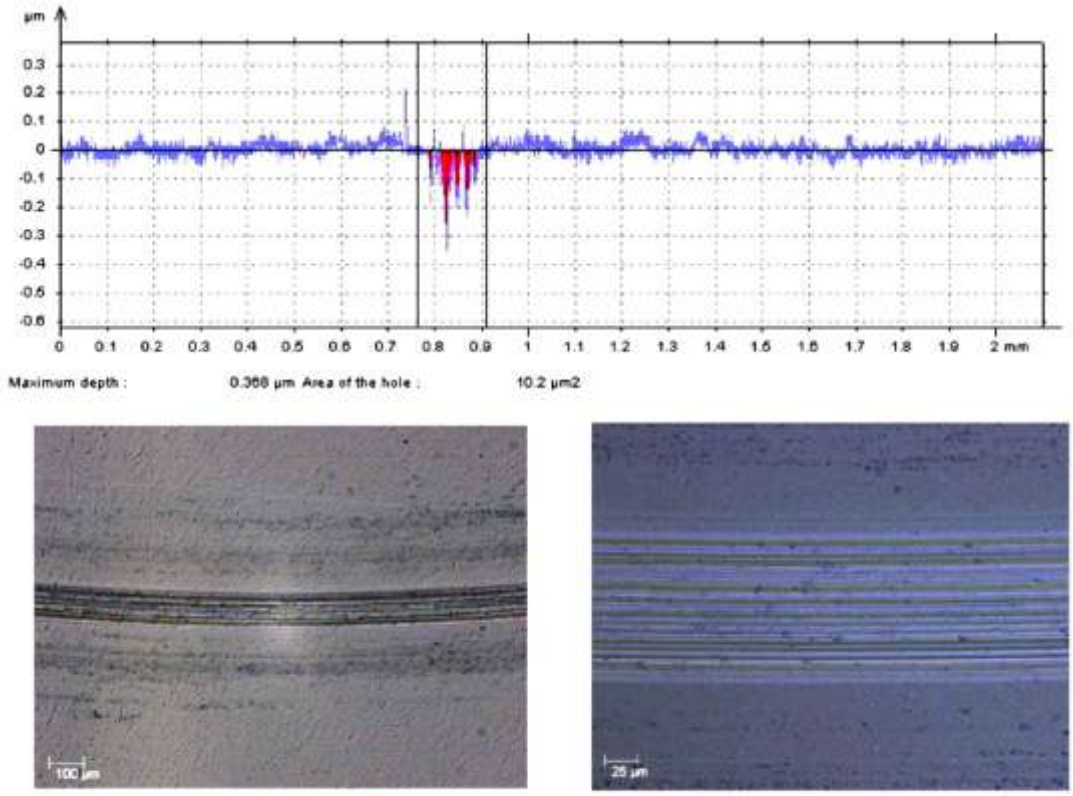

Fig. 9. The wear evaluation for the sample S8—$TiC_{0.77}O_{1.20}N_{1.33}$.

different levels of depth, alternating with film material (Fig. 9). In these cases, after the wear test only the wear dishes affected in depth between 10% and around 35% the film thickness and the substrate is not visible. No spalling phenomenon was observed. This alternating gutters wear aspect could be correlated with the good adherence of the films.

General speaking, with increasing of the oxygen and nitrogen amounts in the films composition, the wear becomes less intense.

For the four representative samples presented in terms of wear behaviours in Figs. 6–9 (samples S1, S3, S5 and S8), the wear rates of the steel-ball counter-bodies were, in the same order: 2.00×10^{-7}, 1.50×10^{-7}, 6.28×10^{-7} and 2.43×10^{-7} $mm^3/N\,m$. Although the mass loss for all the balls is almost the same and insignificant, a higher wear rate can be observed for the ball which worked against sample S5 (the maximum worn sample). This difference could be explained if we take into consideration the early spalling process of the coating and the direct intense contact between the ball and the substrate surface.

The weak point of this study is related to the nonexistent SEM micrographs of wear tracks. However, taking into account the contact arrangement (high contact pressure and the existing of wear track) it is credible to discuss, for all the tests, about a more or less intense abrasive wear mechanism. In fact, owing to the tribometer design is expected that the wear debris is trapped in the wear track and provide the abrasive medium.

The apparition of possible wear debris during wear test and of the abrasive wear mechanism more or less intense could be correlated with the friction coefficient and critical adhesion loads. This could be another explanation for the wear behaviour of S5 sample, which revealed the maximum value for friction coefficient and the minimum one for adhesion critical loads.

4. Conclusions

Dark decorative Ti(C,O,N) coatings with different compositions were deposited on high-speed steel by reactive magnetron sputtering technique. Tribological analysis showed that the most performing coatings were obtained using reactive gas flows of (N_2+O_2) between 8 and 10 sccm, and more than 15 sccm respectively. These coatings are characterised in both flow intervals by amorphous structures and, for the first interval, by a maximum amount of carbon, and for the second one, for maximum contents of oxygen and nitrogen. On the one hand, both the amorphous structure and the high amount of C could influence the tribological behaviour of the coatings, resulting in low friction coefficients and a low wear rates. On the other hand, closer tribological results could be obtained for amorphous structures and high enough contents of oxygen and nitrogen. In this last case, it is expected the developing of poorly crystallised oxide structures, which could play a positive influence on coatings adherence behaviour and tribological properties. Taking into account the decorative aim of these black coatings and the fact that the pure black tones were reached if the oxygen and nitrogen contents

increased [13], from a tribological point of view the recommendation is to use reactive gas flows between 16 and 18 sccm.

Acknowledgements

The authors thank the Portuguese Science Foundation "Fundação para a Ciência e Tecnologia" of Portugal for the post-doctorate Grant SFRH/BPD/27114/2006 and Project PTDC/CTM/69362/2006. The author Daniel Munteanu thanks to CSM Instruments S.A. (CH-2034 Peseux, Switzerland) for the contribution at the tribological tests. The co-author Jean Marie Chappé thanks also to Fundação para a Ciência e Tecnologia for the post-doc Grant SFRH/BBD/27114/2006. The co-author Dida Constantin thanks to Sectorial Operational Programme Human Resources Development (SOP HRD), financed from the European Social Found and by the Romanian Government under the contract number POSDRU/88/1.5/S/59321.

References

[1] Martin N, Banakh O, Santo AME, Springer S, Sanjinés R, Takadoum J, et al. Correlation between processing and properties of TiO_xN_y thin films sputter deposited by the reactive gas pulsing technique. Appl Surf Sci 2001;185:123–33.

[2] Vaz F, Carvalho P, Cunha L, Rebouta L, Moura C, Alves E, et al. Property change in ZrN_xO_y thin films: effect of the oxygen fraction and bias voltage. Thin Solid Films 2004;469–470:11–7.

[3] Vaz F, Cerqueira P, Rebouta L, Nascimento SMC, Alves E, Goudeau Ph, et al. Structural, optical and mechanical properties of coloured TiN_xO_y thin films. Thin Solid Films 2004;447–448:449–54.

[4] Carvalho P, Vaz F, Rebouta L, Cunha L, Tavares CJ, Moura C, et al. Structural, electrical, optical and mechanical characterizations of decorative ZrO_xN_y thin films. J Appl Phys 2005;98(2):023715.

[5] Aravinda CL, Bera P, Jayaram V, Sharma AK, Mayanna SM. Characterization of electrochemically deposited Cu–Ni black coatings. Mater Res Bull 2002;37(3):397–405.

[6] Cui G, Li N, Li D, Zheng J, Wu Q. The physical and electrochemical properties of electroless deposited nickel–phosphorus black coatings. Surf Coat Technol 2006;200:6808–14.

[7] Hollstein F, Louda P. Bio-compatible low reflective coatings for surgical tools using reactive d.c.-magnetron sputtering and arc evaporation—a comparison regarding steam sterilization resistance and nickel diffusion. Surf Coat Technol 1999;120–121:672–81.

[8] Stüber M, Ulrich S, Leiste H, Kratzsch A, Holleck H. Graded layer design for stress-reduced and strongly adherent superhard amorphous carbon films. Surf Coat Technol 1999;116–119:591–8.

[9] Stanishevsky A, Lappalainen R. Tribological properties of composite Ti(N,O,C) coatings containing hard amorphous carbon layers. Surf Coat Technol 2000;123:101–5.

[10] Sobiecki JR, Mankowski P, Wierzchon T. Increased wear and corrosion resistance of Ti(NCO) layers by annealing in a nitrogen plasma atmosphere. Vacuum 2002;68:105–11.

[11] Hsieh JH, Wu W, Li C, Yu CH, Tan BH. Deposition and characterization of Ti(C,N,O) coatings by unbalanced magnetron sputtering. Surf Coat Technol 2003;163–164:233–7.

[12] Chappé JM, Fernandes AC, Cunha L, Moura C, Vaz F, Martin N, et al. TiN based decorative coatings: colour change by addition of C and O. J Optoel Adv Mater 2008;10:900.

[13] Chappé JM, Vaz F, Cunha L, Moura C, Marco de Lucas MC, Imhoff L, et al. Development of dark Ti(C,O,N) coatings prepared by reactive sputtering. Surf Coat Technol 2008;203:804–7.

[14] Azushima A, Tanno Y, Iwata H, Aoki K. Coefficients of friction of TiN coatings with preferred grain orientations under dry condition. Wear 2008;265(7–8):1017–22.

[15] Jin G, Xu B, Wang H, Li Q, Wei S. Investigation on the formation and wear resistance of TiC coatings. Mater Sci Eng A 2006;435–436:355–9.

[16] Zeghni AE, Hashmi MSJ. Comparative wear characteristics of TiN and TiC coated and uncoated tool steel. J Mater Process Tech 2004;155–156:1923–6.

[17] Bhushan B, Gupta BK. Handb. Tribol. 1992:14. 50.

[18] Seitzman LE. An overview of advanced surface engineering technologies for protection against wear. In: Srivasta A, Clayton C, Hirvonen J, editors. Advances in coating technologies for corrosion and wear resistance coatings; 1995. p. 13–25.

[19] Kickel J, Shuaib AN, Yilbas BS, Nizam SM. Evaluation of the wear of the plasma nitrided and TiN coated HSS drills using conventional and Micro-PIXE technique. Wear 2000;234:155–67.

[20] Fernandes AC, Vaz F, Cunha L, Parreira NMG, Cavaleiro A, Goudeau Ph, et al. The influence of structure changes in the properties of TiC_xO_y decorative thin films. Thin Solid Films 2007;515:5424–9.

[21] Zhang S, Lam Bui X, Jiang J, Li X. Microstructure and tribological properties of magnetron sputtered nc-TiC/a-C nanocomposite. Surf Coat Technol 2005;198(1–3):206–11.

[22] Zhu L, He J, Yan DR, Xiao LS, Dong YC, Xue DC, et al. Titanium carbonitride thick coating prepared by plasma spray synthesis and its tribological properties. Chin. Sci. Bull. 2007;52(13):1849–55.

[23] Seidel F, Stock HR, Mayr P. Carbon, nitrogen and oxygen implantation into TiN coatings. Surf Coat Technol 1998;108–109:271–5.

[24] Mathew MT, Ariza E, Rocha LA, Fernandes AC, Vaz F, TiC_xO_y thin films for decorative applications: tribocorrosion mechanisms and synergism. Tribol Int 2008;41:603–15.

[25] Shi Y, Peng H, Xie Y, Xie G, Zhao C, Li S. Plasma CVD of hard coatings Ti(CNO) using metallo-organic compound $Ti(OC_3H_7)_4$. Surf Coat Technol 2000;132:26–30.

[26] Olteanu C, Munteanu D, Munteanu A, Ionescu C, Chappé JM, Cunha L, et al. Tribological characterization of magnetron sputtered Ti(C,O,N) thin films. Int J Mater Prod Tech 2010;39:186–94.

[27] Rocha LA, Ariza E, Ferreira J, Vaz F, Ribeiro E, Rebouta L, et al. Structural and corrosion behaviour of stoichiometric and substoichiometric TiN thin films. Surf Coat Technol 2004;180–181:158–63.

[28] Fonseca C, Vaz F, Barbosa MA. Electrochemical behaviour of titanium coated stainless steel by r.f.sputtering in synthetic sweat solutions for electrode applications. Corros Sci 2004;46:3005–18.

[29] Gu J-D, Chen P-L. Investigation of the corrosion resistance of ZrCN hard coatings fabricated by advanced controlled arc plasma deposition. Surf Coat Technol 2006;200:3341–6.

[30] Mitterer C, Ott HM, Komenda-Stallmaier J, Schmolz P, Werner WSM, Stori H. Sputtered decorative hard coatings within the system LaB_6–ZrB_2. J Alloy Compd 1996;239:183–92.

[31] Vaz F, Cerqueira P, Rebouta L, Nascimento SMC, Alves E, Goudeau Ph, et al. Preparation of magnetron sputtered TiN_xO_y thin films. Surf Coat Technol 2003;174–175:197–203.

[32] Dimigen H, Klages CP. Microstructure and wear behavior of metal-containing diamond-like coatings. Surf Coat Technol 1991;49:543–7.

[33] Persson BNJ, Albohr O, Mancosu F, Peveri V, Samoilov VN, Sivebaek IM. On the nature of the static friction, kinetic friction and creep. Wear 2003;254:835–51.

[34] Scopel VL, Fantini MCA, Alayo MI, Pereyra I. Local structure and bonds of amorphous silicon oxynitride thin films. Thin Solid Films 2002;413:59–64.

[35] Kazemeini MH, Berezin AA, Fukuhara N. Formation of thin TiN_xO_y films by using a hollow cathode reactive DC sputtering system. Thin Solid Films 2000;372:70–7.

[36] Chappé JM, Gavoille J, Martin N, Lintymer J, Takadoum J. Substrate temperature and water vapour effects on structural and mechanical properties of TiO_xN_y coatings. J Mater Sci 2006;41:5639–45.

[37] Colorimetry, vol. 15. CIE Publ. (Commission Internationale de L'Éclairage); 1971.

[38] Recommendations on uniform color spaces. Difference–difference equations, psychometric color terms, vol. 2-70. CIE Publication (Commission Internationale de L'Éclairage); 1978. p. 15.

[39] Zehnder T, Patscheider J. Nanocomposite TiC/a-C:H hard coatings deposited by reactive PVD. Surf Coat Technol 2000;133–134:138–44.

[40] Gulbinski W, Mathur S, Shen H, Suszko T, Gilewicz A, Warcholinski B. Evaluation of phase, composition, microstructure and properties in TiC/a-C:H thin films deposited by magnetron sputtering. Appl Surf Sci 2005;239:302–10.

[41] Martinez-Martinez D, Lopez-Cartes C, Fernandez A, Sanchez-Lopez JC. Influence of the microstructure on the mechanical and tribological behavior of TiC/a-C nanocomposite coatings. Thin Solid Films 2009;517:1662–71.

[42] Jia Q, Zhang Y, Wu Z, Zhang P. Tribological properties of anatase TiO_2 sol–gel films controlled by mutually soluble dopants. Tribol Lett 2007;26:19–24.